First Observation of Large Missing-Momentum $(e, e'p)$ Cross-Section Scaling and the onset of Correlated-Pair Dominance in Nuclei

I. Korover,[1,*] A.W. Denniston,[1,*] A. Kiral,[1] A. Schmidt,[3] A. Lovato,[6] N. Rocco,[7] A. Nikolakopoulos,[7] L.B. Weinstein,[4] E. Piasetzky,[2] O. Hen,[1,†] M.J. Amaryan,[4] Giovanni Angelini,[3] H. Atac,[45] N.A. Baltzell,[5] L. Barion,[21] M. Battaglieri,[5,23] I. Bedlinskiy,[34] Fatiha Benmokhtar,[16] A. Bianconi,[48,27] L. Biondo,[23,26,49] A.S. Biselli,[17,10] F. Bossù,[12] S. Boiarinov,[5] W.J. Briscoe,[3] D. Bulumulla,[4] V.D. Burkert,[5] D.S. Carman,[5] J.C. Carvajal,[19] M. Caudron,[28] P. Chatagnon,[28] T. Chetry,[33] G. Ciullo,[21,18] L. Clark,[50] P.L. Cole,[32,11,5] M. Contalbrigo,[21] G. Costantini,[48,27] A. D'Angelo,[24,42] N. Dashyan,[54] R. De Vita,[23] M. Defurne,[12] A. Deur,[5] S. Diehl,[39,14] C. Djalali,[38] M. Duer,[55] R. Dupre,[28] H. Egiyan,[5] M. Ehrhart,[6] A. El Alaoui,[46] L. El Fassi,[33] L. Elouadrhiri,[5] P. Eugenio,[20] S. Fegan,[51] R. Fersch,[13] A. Filippi,[25] G. Gavalian,[5,35] Y. Ghandilyan,[54] G.P. Gilfoyle,[41] F.X. Girod,[5] A.A. Golubenko,[43] R.W. Gothe,[44] K.A. Griffioen,[53] M. Guidal,[28] L. Guo,[19,5] K. Hafidi,[6] H. Hakobyan,[46,54] M. Hattawy,[4] T.B. Hayward,[14] D. Heddle,[13,5] K. Hicks,[38] A. Hobart,[28] M. Holtrop,[35] C.E. Hyde,[4] Y. Ilieva,[44,3] D.G. Ireland,[50] E.L. Isupov,[43] H.S. Jo,[31] K. Joo,[14] S. Joosten,[6] D. Keller,[52] A. Khanal,[19] M. Khandaker,[37,‡] A. Kim,[14] W. Kim,[31] A. Kripko,[39] V. Kubarovsky,[5,40] L. Lanza,[24] M. Leali,[48,27] P. Lenisa,[21,18] K. Livingston,[50] I .J .D. MacGregor,[50] D. Marchand,[28] L. Marsicano,[23] V. Mascagna,[47,27,§] B. McKinnon,[50] S. Migliorati,[48,27] M. Mirazita,[22] V. Mokeev,[5,43] C. Munoz Camacho,[28] P. Nadel-Turonski,[5] K. Neupane,[44] S. Niccolai,[28] G. Niculescu,[30] T. R. O'Connell,[14] M. Osipenko,[23] A.I. Ostrovidov,[20] P. Pandey,[4] M. Paolone,[36] L.L. Pappalardo,[21,18] R. Paremuzyan,[5] E. Pasyuk,[5] O. Pogorelko,[34] M. Pokhrel,[4] J. Poudel,[4] J.W. Price,[8] Y. Prok,[4,52] B.A. Raue,[19,5] Trevor Reed,[19] M. Ripani,[23] J. Ritman,[29] A. Rizzo,[24,42] G. Rosner,[50] P. Rossi,[5] J. Rowley,[38] F. Sabatié,[12] R.A. Schumacher,[10] E.P. Segarra,[1] Y.G. Sharabian,[5] E.V. Shirokov,[43] U. Shrestha,[14] O. Soto,[22] N. Sparveris,[45] S. Stepanyan,[5] I.I. Strakovsky,[3] S. Strauch,[44,3] R. Tyson,[50] M. Ungaro,[5,40] L. Venturelli,[48,27] H. Voskanyan,[54] A. Vossen,[15,5] E. Voutier,[28] Kevin Wei,[14] X. Wei,[5] R. Wishart,[50] M.H. Wood,[9,44] B. Yale,[53] N. Zachariou,[51] J. Zhang,[52] and Z.W. Zhao[15]

(The CLAS Collaboration)

[1] *Massachusetts Institute of Technology, Cambridge, Massachusetts 02139, USA*
[2] *School of Physics and Astronomy, Tel Aviv University, Tel Aviv 69978, Israel*
[3] *The George Washington University, Washington DC 20052, USA*
[4] *Old Dominion University, Norfolk, Virginia 23529, USA*
[5] *Thomas Jefferson National Accelerator Facility, Newport News, Virginia 23606, USA*
[6] *Physics Division, Argonne National Laboratory, Lemont, Illinois 60439, USA*
[7] *Theoretical Physics Department, Fermi National Accelerator Laboratory , P.O. Box 500, Batavia, Illinois 60510, USA*
[8] *California State University, Dominguez Hills, Carson, CA 90747*
[9] *Canisius College, Buffalo, NY*
[10] *Carnegie Mellon University, Pittsburgh, Pennsylvania 15213*
[11] *Catholic University of America, Washington, D.C. 20064*
[12] *IRFU, CEA, Université Paris-Saclay, F-91191 Gif-sur-Yvette, France*
[13] *Christopher Newport University, Newport News, Virginia 23606*
[14] *University of Connecticut, Storrs, Connecticut 06269*
[15] *Duke University, Durham, North Carolina 27708-0305*
[16] *Duquesne University, 600 Forbes Avenue, Pittsburgh, PA 15282*
[17] *Fairfield University, Fairfield CT 06824*
[18] *Universita' di Ferrara , 44121 Ferrara, Italy*
[19] *Florida International University, Miami, Florida 33199*
[20] *Florida State University, Tallahassee, Florida 32306*
[21] *INFN, Sezione di Ferrara, 44100 Ferrara, Italy*
[22] *INFN, Laboratori Nazionali di Frascati, 00044 Frascati, Italy*
[23] *INFN, Sezione di Genova, 16146 Genova, Italy*
[24] *INFN, Sezione di Roma Tor Vergata, 00133 Rome, Italy*
[25] *INFN, Sezione di Torino, 10125 Torino, Italy*
[26] *INFN, Sezione di Catania, 95123 Catania, Italy*
[27] *INFN, Sezione di Pavia, 27100 Pavia, Italy*
[28] *Universit'e Paris-Saclay, CNRS/IN2P3, IJCLab, 91405 Orsay, France*
[29] *Institute fur Kernphysik (Juelich), Juelich, Germany*
[30] *James Madison University, Harrisonburg, Virginia 22807*
[31] *Kyungpook National University, Daegu 41566, Republic of Korea*

[32]Lamar University, 4400 MLK Blvd, PO Box 10046, Beaumont, Texas 77710
[33]Mississippi State University, Mississippi State, MS 39762-5167
[34]National Research Centre Kurchatov Institute - ITEP, Moscow, 117259, Russia
[35]University of New Hampshire, Durham, New Hampshire 03824-3568
[36]New Mexico State University, PO Box 30001, Las Cruces, NM 88003, USA
[37]Norfolk State University, Norfolk, Virginia 23504
[38]Ohio University, Athens, Ohio 45701
[39]II Physikalisches Institut der Universitaet Giessen, 35392 Giessen, Germany
[40]Rensselaer Polytechnic Institute, Troy, New York 12180-3590
[41]University of Richmond, Richmond, Virginia 23173
[42]Universita' di Roma Tor Vergata, 00133 Rome Italy
[43]Skobeltsyn Institute of Nuclear Physics, Lomonosov Moscow State University, 119234 Moscow, Russia
[44]University of South Carolina, Columbia, South Carolina 29208
[45]Temple University, Philadelphia, PA 19122
[46]Universidad Técnica Federico Santa María, Casilla 110-V Valparaíso, Chile
[47]Università degli Studi dell'Insubria, 22100 Como, Italy
[48]Universit'a degli Studi di Brescia, 25123 Brescia, Italy
[49]Universit'a degli Studi di Messina, 98166 Messina, Italy
[50]University of Glasgow, Glasgow G12 8QQ, United Kingdom
[51]University of York, York YO10 5DD, United Kingdom
[52]University of Virginia, Charlottesville, Virginia 22901
[53]College of William and Mary, Williamsburg, Virginia 23187-8795
[54]Yerevan Physics Institute, 375036 Yerevan, Armenia
[55]Technische Universität Darmstadt, Fachbereich Physik, Darmstadt, Germany

(Dated: September 7, 2022)

We report the first measurement of x_B-scaling in $(e, e'p)$ cross-section ratios off nuclei relative to deuterium at large missing-momentum of $350 \leq p_{miss} \leq 600$ MeV/c. The observed scaling extends over a kinematic range of $0.7 \leq x_B \leq 1.8$, which is significantly wider than $1.4 \leq x_B \leq 1.8$ previously observed for inclusive (e, e') cross-section ratios. The x_B-integrated cross-section ratios become constant (i.e., scale) beginning at $p_{miss} \approx k_F$, the nuclear Fermi momentum. Comparing with theoretical calculations we find good agreement with Generalized Contact Formalism calculations for high missing-momentum (> 375 MeV/c), suggesting the observed scaling results from interacting with nucleons in short-range correlated (SRC) pairs. For low missing-momenta, mean-field calculations show good agreement with the data for $p_{miss} \leq k_F$, and suggest that contributions to the measured cross-section ratios from scattering off single, un-correlated, nucleons are non-negligible up to $p_{miss} \approx 350$ MeV/c. Therefore, SRCs become dominant in nuclei at $p_{miss} \approx 350$ MeV/c, well above the nuclear Fermi Surface of $k_F \approx 250$ MeV/c.

Atomic nuclei are complex quantum-mechanical systems that account for most of the visible mass in the universe. The complexity of the strong nuclear interaction makes it difficult to use scattering reactions to experimentally probe the detailed distributions of nucleons inside nuclei. Experimental nuclear physicists thus work together with theorists to find measurable reactions that are sensitive to particular aspects of nuclear dynamics.

By using high-energy electron beams to knock out nucleons from nuclei in nearly elastic kinematics, one can learn about the behavior of single nucleons in the nucleus [1]. This behavior can be generally explained by nucleons moving in nuclear shell-model states (e.g. *s*-, *p*-, *d*-, ... shells) where the typical nucleon momenta in each shell is smaller than the nuclear Fermi momentum (k_F). Full shell-model calculations improve on this by introducing effective long-ranged correlations between the nucleons [2], which leads to the formation of a nuclear Fermi Surface.

While these models can successfully describe the long-range structure of nuclei, they do not describe the explicit high-resolution effects of short-range correlated (SRC) nucleon pairs. Within a high-resolution picture of nuclear dynamics, SRC pairs arise when two nucleons get so close to each other that the short-range nuclear interaction between them is much stronger than the effective long-ranged nuclear mean field due to their interactions with all the other nucleons in the nucleus [3, 4].

SRCs have been clearly identified in data using large momentum-transfer nucleon knockout reactions [5–9]. They are characterized by a high (greater than k_F) relative momentum between the nucleons of the pair and are predominantly proton-neutron pairs formed due to the action of the spin-dependent tensor part of the strong nuclear interaction [10–13]. They thus deplete the occupancy of single-particle shell-model states (below k_F) and populate high-momentum states [3, 4, 9, 14–16] While shell structures vary among nuclei, SRCs are a universal phenomenon, i.e., they are similar in all nuclei [4, 17–19], varying primarily in their magnitude.

A complete high-resolution microscopic description of atomic nuclei should thus have the nucleus-dependent

mean field and long-ranged nuclear shell model parts as well as explicit nucleus-independent effects of SRC pairs.

Here we study the onset of SRC dominance in semi-inclusive high-energy electron scattering reactions, where we detect the knocked-out proton in addition to the scattered electron, $(e, e'p)$. For the first time in $(e, e'p)$ reactions, we observed scaling in the cross-section ratios of nuclei from carbon to lead relative to deuterium over a broad range in the Bjorken scaling variable, x_B. This scaling substantially extends the kinematical range where SRCs can be identified and studied, as compared with previous inclusive (e, e') measurements. Thereby, they provide direct experimental evidence for the dominance SRCs in the scattering response at high missing momenta, and allow quantifying the onset of this dominance.

Our experiment ran at the Thomas Jefferson National Accelerator Facility. It used a 5.01 GeV electron beam incident on a target system consisting of a deuterium cell followed by an interchangeable solid foil of carbon (C), aluminum (Al), iron (Fe), or lead (Pb) [20]. Scattered electrons and knocked-out protons were identified and measured using the CEBAF Large Acceptance Spectrometer (CLAS) [21] (see supplementary materials for details).

In high-energy scattering, the electron transfers a single virtual photon to the nucleus with momentum $\vec{q}$ and energy ω. In the high-resolution quasielastic (QE) reaction picture, the virtual photon is absorbed by a single nucleon, which gets knocked-out of the nucleus with momentum $\vec{p}_p$. By measuring both the scattered electron and knocked-out proton, i.e. the $(e, e'p)$ reaction, we can determine the missing momentum $\vec{p}_{miss} = \vec{p}_p - \vec{q}$. The reaction is further characterized by the four-momentum transfer $Q^2 = \vec{q}^2 - \omega^2$ and Bjorken scaling variable $x_B = Q^2/2m\omega$ where m is the nucleon mass.

If the knocked-out nucleon does not re-interact as it leaves the nucleus, then $\vec{p}_{miss}$ is equal to the initial momentum of that nucleon. Thus we expect the reaction to be sensitive to mean-field nucleons at low-p_{miss} and to SRCs at high-p_{miss} [22]. In the SRC dominated region, the cross section ratio for any two nuclei should be constant (i.e., independent of p_{miss}) and equal to the relative number of high-momentum nucleons in the two nuclei [4, 9, 14, 23–26]. Thus, by measuring the $(e, e'p)$ cross section ratio for nuclei relative to deuterium for different minimum p_{miss}, we can establish the onset of scaling that corresponds to SRC pair dominance in the nuclear momentum distribution.

To study this, we measured the $(e, e'p)$ reaction in conditions sensitive to the knockout of protons from SRC pairs. We required $Q^2 \geq 1.5$ (GeV/c)^2 and $350 \leq p_{miss} \leq 600$ MeV/c to ensure a high-resolution reaction that can resolve single nucleons in SRC pairs. We further required that the proton be emitted within 25° of the momentum transfer, to ensure that the measured proton was the nucleon that absorbed the virtual photon [28, 29].

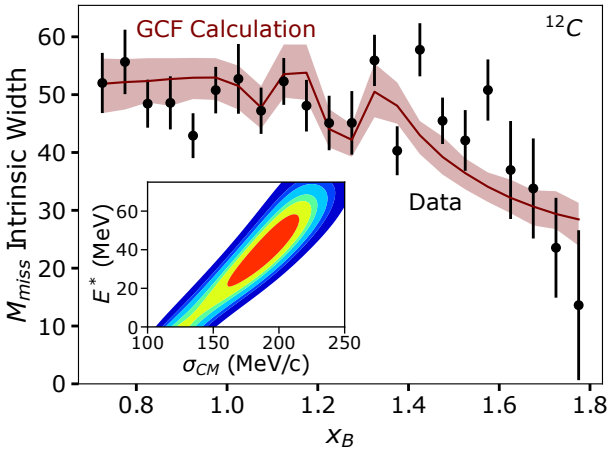

FIG.1: The intrinsic width of the ^{12}C missing mass (M_{miss}) distribution, plotted vs x_B. Black points show the data. The red curve and uncertainty band shows an SRC based Generalized Contact Formalism (GCF) calculation[19, 27]. The two main model parameters of the calculation, namely SRC pair CM momentum distribution width σ_{CM} and the residual $A-2$ system excitation energy E^*, are fit to the data. Data error bars and calculation error band show the total uncertainty (statistical + systematical) at the 1σ or 68% confidence level. Inset: The resulting confidence intervals of the correlation between the fitted values of σ_{CM} and E^*. The inner region (red) shows the 1σ (68%) confidence region with each region increasing the confidence by an additional 1σ. The observed agreement between the data and GCF calculation, and the agreement of the fitted model parameters with previous extractions, show the measured $(e, e'p)$ events are consistent with resulting from the hard breakup of SRC pairs.

We suppressed inelastic (non-QE) scattering events by requiring M_{miss}, the missing mass for $(e, e'p)$ scattering from a two-nucleon pair at rest, to be smaller than the nucleon mass (m) plus pion mass (m_π), $0.8 \leq M_{miss} \leq m + m_\pi = 1.08$ GeV/c^2. In non-QE reactions the momentum transferred to undetected particles (e.g., pions) shifts the direction of $\vec{p}_{miss}$. Therefore such events will have a larger $\theta_{\vec{p}_{miss},\vec{q}}$, the angle between $\vec{p}_{miss}$ and $\vec{q}$. We thus further suppressed the small non-QE tail below $M_{miss} = 1.08$ GeV/c^2 by observing that the measured $\theta_{\vec{p}_{miss},\vec{q}}$ distribution has two maxima, corresponding to QE and non-QE scattering, and selecting events in the $\theta_{\vec{p}_{miss},\vec{q}}$ QE peak. See Figs. S1 and S2 and supplementary materials for details.

We tested our identification of scattering from protons in SRC pairs by comparing the measured width of the M_{miss} peak with that calculated using the Generalized Contact Formalism (GCF) model for SRC pairs (see Fig. 1) [8, 19, 27, 29–31]. This width depends on the CLAS resolution and on the SRC pair center of mass (CM) motion. We corrected for the effects of the CLAS resolution by subtracting the deuterium M_{miss}

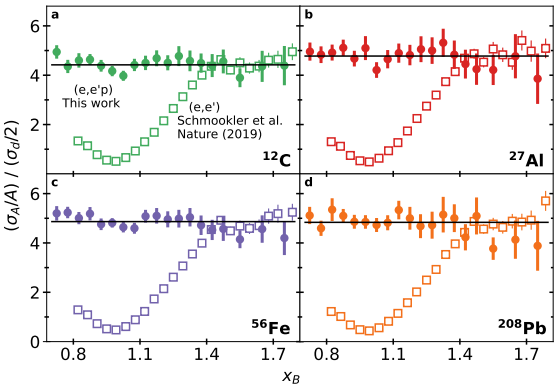

FIG. 2: Measured $(e, e'p)$ per nucleon cross-section ratios for $350 \leq p_{miss} \leq 600$ MeV/c for carbon, aluminum, iron and lead relative to deuterium as function of x_B. Open squares are the inclusive (e, e') per nucleon cross section ratios of Ref. [26]. The horizontal lines show the average (e, e') cross section ratio for $1.45 \leq x_B \leq 1.8$ [26]. Error bars show the data uncertainty (statistical plus point-to-point systematical) at the 1σ or 68% confidence level. Overall $(e, e'p)$ systematic uncertainties of 10% (C) to 15% (Pb) are not shown.

peak width from that of ^{12}C to get the intrinsic width: $\sigma_{int}^{^{12}C} = \sqrt{(\sigma_{exp}^{^{12}C})^2 - (\sigma_{exp}^{d})^2}$.

The measured x_B dependence of $\sigma_{int}^{^{12}C}$ agrees well with a GCF calculation that assumes electron scattering from nucleons in SRC pairs with a realistic Gaussian CM momentum distribution [32], as was done in Refs. [8, 27, 29]. The calculation accounts for the CLAS detector acceptance and resolution and our event selection cuts. The width of the CM momentum distributions, σ_{CM}, and the excitation energy of the residual nuclear system after the SRC breakup, E^*, were the only two free parameters used in the calculation and were determined from a fit of the calculation to the data (see inset of Fig. 1). For σ_{CM} the fitted values of $160 - 210$ MeV/c $(125 - 220)$ at 68% (90%) confidence agree well with previous direct measurements [8, 32]. For E^*, while not previously measured, the fitted values of $20 - 55$ MeV $(0 - 70$ MeV) at 68% (90%) confidence are consistent with those used by previous analyses [29]. The sensible values of the resulting fit parameters and the agreement between the x_B dependence of the GCF calculation and the data further support our interpretation of the data as dominated by scattering off SRC pairs.

Using the selected event samples, we extracted the $(e, e'p)$ cross section ratios for scattering off the solid targets relative to deuterium. We first divided the ratio of the measured numbers of events for a given target to deuterium with the ratio of the experimentally determined integrated luminosities to obtain the normalized-yield ratios. We then determined the cross section ratios by correcting the normalized-yield ratios for attenuation of the outgoing protons as they traverse the different nuclei [33], electron radiation effects, and the small difference in the CLAS acceptance for detecting particles emitted from the deuterium and the solid targets. At the large Q^2 of this measurement, the attenuation correction is less sensitive to the initial nucleon momenta and therefore both mean-field and SRC breakup reactions have the same attenuation [33]. Acceptance effects were calculated using the CLAS detector simulation [34] and an electron scattering reaction event generator based on the GCF as applied in previous studies [27, 29] (see supplementary materials for details).

Figure 2 shows the per nucleon $(e, e'p)$ cross section ratios for $350 \leq p_{miss} \leq 600$ MeV/c for carbon, aluminum, iron, and lead relative to deuterium as a function of x_B. The $(e, e'p)$ ratios scale (i.e., are constant) for all four nuclei over the entire measured x_B range. This implies that the reaction is probing similar nuclear configurations in the measured nuclei and in deuterium. As the deuteron is a simple proton-neutron correlated two-body system, we interpret this high missing-momentum scaling as observation of deuteron-like proton-neutron SRC pairs in nuclei. The cross-section ratio is thus a measure of their relative abundance.

This interpretation is supported by the consistency between our measured $(e, e'p)$ cross section ratios and previously measured inclusive (e, e') scattering cross section ratios at similar Q^2 and at $x_B \geq 1.5$ [14, 23–26] (see open symbols in Fig. 2). As the inclusive scaling onset at $x_B \approx 1.5$ has been attributed to scattering off nucleons with momenta greater than ~ 275 MeV/c [14, 35], it is also associated with scattering off nucleons in deuteron-like proton-neutron SRC pairs, formed by the strong tensor interaction [23, 26] (see supplementary materials for details). Proton detection extends the cross-section ratio plateau down to $x_B = 0.7$, providing a new experimental tool to study the transition to SRC dominance in nuclei over a broad range in x_B.

We next examined how this scaling depends on the minimum p_{miss} range of the data. Figure 3 shows the per nucleon $(e, e'p)$ cross section ratios for the measured nuclei relative to deuterium as a function of x_B for different minimum p_{miss}. For all nuclei, the curve for $p_{miss}^{min} = 0$ are similar to the inclusive data of Schmookler et al. [26], with a plateau for $x_B \geq 1.5$ and a minimum at $x_B \approx 1$. As p_{miss}^{min} increases, this minimum fills in. For $p_{miss}^{min} \gtrsim 200 - 250$ MeV/c, it is completely filled in and the $(e, e'p)$ cross section ratio scales over the full measured x_B range of 0.7 to 1.8. This indicates that short-range interactions become dominant at around $k_F \approx 220 - 260$ MeV/c [36], as expected.

To better quantify this transition, Figure 4 shows the p_{miss} dependence of the $(e, e'p)$ cross section ratio for the different nuclei relative to deuterium, integrated over the scaling regions of $0.7 \leq x_B \leq 1.8$. The measured cross section ratio for carbon ($k_F \approx 220$ MeV/c), alu-

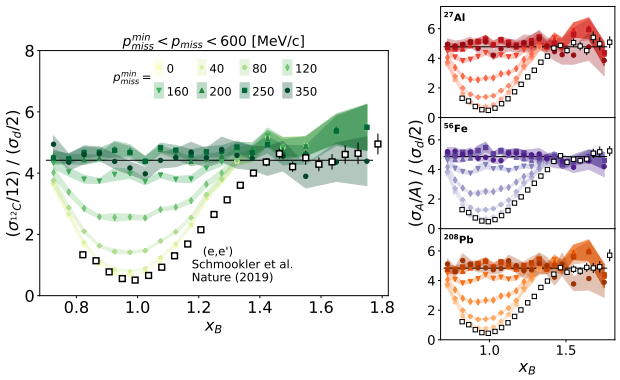

FIG. 3: The per-nucleon cross-section ratios for carbon (left), aluminum, iron and lead (right) to deuterium as a function of x_B. Full symbols with different colors indicate different lower limits of the p_{miss} integration. The upper p_{miss} limit is fixed at 600 MeV/c. The colored bands mark the statistical plus point-to-point systematical uncertainty of the data at the $\pm 1\sigma$ or 68% confidence level. Overall systematic uncertainties of 10–15% are not shown. Open black squares show the inclusive (e, e') per nucleon cross-section ratios of Ref. [26]. The horizontal line shows the average (e, e') cross section ratio for $1.45 \leq x_B \leq 1.8$ [26].

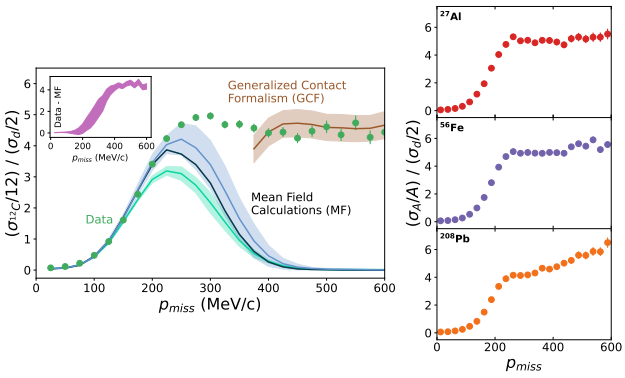

FIG. 4: The per nucleon $(e, e'p)$ cross-section ratios for different nuclei to deuterium as a function of p_{miss}, integrated over $0.7 \leq x_B \leq 1.8$. Filled circles show the data. The teal, black, and azure lines show the calculated cross sections obtained using QMC (teal), IPSM (black), and Skryme (azure) based one-body mean-field models for nucleon distributions in carbon. The brown line shows a GCF calculation for SRC nucleons in carbon. Data error bars and the widths of the bands around the calculation lines show their uncertainties (statistical plus point-to-point systematical) at the 1σ or 68% confidence level. Overall data systematic data uncertainties of 10–15% are not shown. The insert shows the result of subtracting the mean-field calculations from the carbon data.

minum ($k_F \approx 235$ MeV/c), and iron ($k_F \approx 260$ MeV/c) all become flat starting around the Fermi momentum at $p_{miss} \approx 250$. The lead ratio shows a similar transition but does not fully plateau, possibly owing to its much larger neutron-to-proton ratio or to increased final state interactions due to its larger size.

We thus conclude that the data indicate the existence of a clear transition in the nuclear response around the nuclear Fermi momentum, resulted by the onset of the SRC dominance at high-momenta.

Focusing on the carbon nucleus, where theoretical calculations are readily available, we find that the high-p_{miss} data are in excellent agreement with an asymptotic GCF calculation of the cross-section ratio (brown band in Fig. 4, left panel). The calculation was done using a factorized plane-wave impulse approximation (PWIA) for the scattering reaction, with SRC-pair spectral functions calculated using the GCF [37] and transparency and single-charge exchange corrections as done in Ref. [27, 29, 38] (see supplementary materials for details). The SRC-pair abundance parameters used by the GCF calculation were all previously determined by $ab-initio$ many-body theoretical calculations [19], offering additional support to our identification of QE scattering events and the dominance of interacting with nucleons in SRC pairs at high-p_{miss}.

Lastly, we estimate the possible contribution of single-nucleon (one-body) states to the measured cross-section ratio around k_F, to assess their impact on the observed SRC scaling onset. We examined three calculations using different single-nucleon spectral functions: (1) Independent particle shell-model with Woods-Saxon potential [39, 40], (2) Skryme model using 5 different functionals [41, 42] and (3) new Quantum Monte-Carlo (QMC) many-body calculations of the overlap between the ^{12}C and ^{11}B+proton wave functions (see supplementary materials for details). For the latter, we added the contributions from both the ground state and a range of ^{11}B excited states to include a wide range of mean-field, single-nucleon states. These models each assume very different underlying single-body nuclear dynamics, and thus the spread in their results offers a general measure for the model dependence of the single-body mean-field contribution.

The resulting calculated one-body mean-field contributions to the C/d $(e, e'p)$ cross section ratio are shown in Figure 4, left panel. The calculations were done using the same factorized PWIA scheme as for the GCF calculation, only using mean-field spectral functions. The IPSM and Skryme calculations are re-normalized (quenched) to agree with our low-p_{miss} ($\leq$ 150 MeV/c) high-Q^2 data. This effectively accounts for their lack of single-nucleon strength lost to long- and short-ranged correlations and/or few-body reaction operators that can compensate for it [43]. In contrast, the QMC calculation extracts the underlying single-nucleon states from the fully correlated high-resolution wave function. It thus has fewer than six protons in its mean-field orbitals and does not require additional quenching.. The agreement of the QMC calculation with the low-p_{miss} data thus con-

firms the completeness of the calculation.

The different single-nucleon calculations are similar and all show the existence of residual single nucleon contributions above k_F. We subtracted the calculated one-body mean-field contribution from the measured cross-section ratio(see the inset in Fig. 4)left. Accounting for these contributions can shift the scaling onset from the purely experimental onset at $\sim k_F$ to a higher value of $\sim$ 350 MeV/c. Such a shift would be consistent with the existence of a nuclear Fermi-surface that accounts for long-range correlations above k_F.

To conclude, the new nuclear scaling measurements presented herein allow isolating interactions with SRC pairs in a substantially-extended kinematical regime. By examining the scaling onset in missing momentum, we observe a universal transition in the scattering response above the nuclear Fermi momentum. Using model dependent estimates for mean field contributions, we see an indication for the onset of full SRC dominance above $\sim$ 350 MeV/c. Detailed theoretical calculations will be able to use our data to fully quantify this mean-field to SRC transition region and to obtain an effective high-resolution description of a wide range of heavy nuclei.

We acknowledge the efforts of the staff of the Accelerator and Physics Divisions at Jefferson Lab that made this experiment possible. The analysis presented here was carried out as part of the Jefferson Lab Hall B data-mining project supported by the U.S. Department of Energy (DOE). The research was also supported by the National Science Foundation, the Israel Science Foundation, the Pazi Foundation, the Chilean Comisión Nacional de Investigación Científica y Tecnológica, the French Centre National de la Recherche Scientifique and Commissariat a l'Energie Atomique, the French–American Cultural Exchange, the Italian Istituto Nazionale di Fisica Nucleare, the National Research Foundation of Korea, and the UK Science and Technology Facilities Council. Jefferson Science Associates operates the Thomas Jefferson National Accelerator Facility for the DOE, Office of Science, Office of Nuclear Physics under contract DE-AC05-06OR23177.

* Equal Contribution
† Contact Author hen@mit.edu
‡ Current address:Idaho State University, Pocatello, Idaho 83209
§ Current address:Universit'a degli Studi di Brescia, 25123 Brescia, Italy

[1] J. Kelly, Adv. Nucl. Phys. **23**, 75 (1996).
[2] W. H. Dickhoff and C. Barbieri, Prog. Part. Nucl. Phys. **52**, 377 (2004), nucl-th/0402034.
[3] L. Frankfurt and M. Strikman, Phys. Rep. **160**, 235 (1988).
[4] C. Ciofi degli Atti, Phys. Rept. **590**, 1 (2015).
[5] A. Tang et al., Phys. Rev. Lett. **90**, 042301 (2003), nucl-ex/0206003.
[6] R. Subedi et al., Science **320**, 1476 (2008), 0908.1514.
[7] O. Hen et al., Science **346**, 614 (2014), 1412.0138.
[8] M. Patsyuk et al. (BM@N), Nature Physics **17**, 693 (2021), 2102.02626.
[9] O. Hen, G. A. Miller, E. Piasetzky, and L. B. Weinstein, Rev. Mod. Phys. **89**, 045002 (2017).
[10] R. Schiavilla, R. B. Wiringa, S. C. Pieper, and J. Carlson, Phys. Rev. Lett. **98**, 132501 (2007).
[11] M. M. Sargsian, T. V. Abrahamyan, M. I. Strikman, and L. L. Frankfurt, Phys. Rev. C **71**, 044615 (2005).
[12] M. Alvioli, C. Ciofi degli Atti, and H. Morita, Phys. Rev. Lett. **100**, 162503 (2008).
[13] T. Neff, H. Feldmeier, and W. Horiuchi, Phys. Rev. C **92**, 024003 (2015).
[14] K. Egiyan et al. (CLAS Collaboration), Phys. Rev. Lett. **96**, 082501 (2006).
[15] S. Paschalis, M. Petri, A. O. Macchiavelli, O. Hen, and E. Piasetzky, Phys. Lett. B **800**, 135110 (2020), 1812.08051.
[16] J. Ryckebusch, W. Cosyn, T. Vieijra, and C. Casert, Phys. Rev. C **100**, 054620 (2019), 1907.07259.
[17] C. Ciofi degli Atti and S. Simula, Phys. Rev. C **53**, 1689 (1996).
[18] J. Ryckebusch, M. Vanhalst, and W. Cosyn, Journal of Physics G: Nuclear and Particle Physics **42**, 055104 (2015).
[19] R. Cruz-Torres et al., Nature Physics **17**, 306 (2020), 1907.03658.
[20] H. Hakobyan et al., Nucl. Instrum. Meth. **A592**, 218 (2008).
[21] B. A. Mecking et al., Nucl. Instrum. Meth. **A503**, 513 (2003).
[22] M. Duer et al. (CLAS Collaboration), Nature **560**, 617 (2018).
[23] L. Frankfurt, M. Strikman, D. Day, and M. Sargsyan, Phys. Rev. C **48**, 2451 (1993).
[24] K. Egiyan et al. (CLAS Collaboration), Phys. Rev. C **68**, 014313 (2003).
[25] N. Fomin et al., Phys. Rev. Lett. **108**, 092502 (2012).
[26] B. Schmookler et al. (CLAS Collaboration), Nature **566**, 354 (2019).
[27] J. Pybus, I. Korover, R. Weiss, A. Schmidt, N. Barnea, D. Higinbotham, E. Piasetzky, M. Strikman, L. Weinstein, and O. Hen, Phys. Lett. B **805**, 135429 (2020), 2003.02318.
[28] O. Hen et al., Science **346**, 614 (2014), 1412.0138.
[29] A. Schmidt et al. (CLAS), Nature **578**, 540 (2020), 2004.11221.
[30] R. Weiss, B. Bazak, and N. Barnea, Phys. Rev. **C92**, 054311 (2015), 1503.07047.
[31] R. Weiss, R. Cruz-Torres, N. Barnea, E. Piasetzky, and O. Hen, Phys. Lett. B **780**, 211 (2018).
[32] E. O. Cohen et al. (CLAS Collaboration), Phys. Rev. Lett. **121**, 092501 (2018), 1805.01981.
[33] M. Duer et al. (CLAS Collaboration), Phys. Lett. **B797**, 134792 (2019), 1811.01823.
[34] E. Wolin, *Clas - geant simulation* (1996), URL `https://www.jlab.org/Hall-B/document/gsim/userguide.html`.
[35] R. Weiss, A. W. Denniston, J. R. Pybus, O. Hen, E. Piasetzky, A. Schmidt, L. B. Weinstein, and N. Barnea, Phys. Rev. C **103**, L031301 (2021), 2005.01621.
[36] E. J. Moniz, I. Sick, R. R. Whitney, J. R. Ficenec, R. D. Kephart, and W. P. Trower, Phys. Rev. Lett. **26**, 445

(1971).
[37] R. Weiss, I. Korover, E. Piasetzky, O. Hen, and N. Barnea, Phys. Lett. **B791**, 242 (2019), 1806.10217.
[38] M. Duer et al. (CLAS Collaboration), Phys. Rev. Lett. **122**, 172502 (2019), 1810.05343.
[39] T. O'Neill, W. Lorenzon, P. Anthony, R. Arnold, J. Arrington, E. Beise, J. Belz, P. Bosted, H.-J. Bulten, M. Chapman, et al., Physics Letters B **351**, 87 (1995), ISSN 0370-2693.
[40] N. Makins et al., Phys. Rev. Lett. **72**, 1986 (1994).
[41] M. Waroquier, J. Sau, K. Heyde, P. Van Isacker, and H. Vincx, Phys. Rev. C **19**, 1983 (1979).
[42] E. Chabanat, P. Bonche, P. Haensel, J. Meyer, and R. Schaeffer, Nucl. Phys. A **635**, 231 (1998), [Erratum: Nucl.Phys.A 643, 441–441 (1998)].
[43] A. J. Tropiano, S. K. Bogner, and R. J. Furnstahl, Phys. Rev. C **104**, 034311 (2021), 2105.13936.